

Highlights of Joint Research

Synchrotron Radiation Laboratory

The Synchrotron Radiation Laboratory (SRL) was established in 1975 as a research group dedicating to solid state physics using synchrotron radiation. In 1989, the SRL started to hold the Tsukuba branch, a branch laboratory in the Photon Factory (PF), High Energy Accelerator Research Organization (KEK). The SRL consists of the accelerator physics group and the solid state spectroscopy group. The members of the accelerator group have been carrying out research works on the accelerator physics and developing various new accelerator related technology in collaboration with other SR facilities. The spectroscopy group has been not only serving users at the Tsukuba branch with technical supports and advices, but also carrying out their own research works on advanced solid state spectroscopy. SRL maintains an undulator called Revolver, two beamlines and three experimental stations; BL-18A for angle-resolved photoemission spectroscopy with SCIENTA SES100 energy analyser and undulator beamlines, BL-19A and BL-19B, for spin-resolved photoelectron spectroscopy and soft X-ray emission spectroscopy experiments, respectively. In 2008, the new spin detector utilizing very low energy electron diffraction (VLEED) has started its normal operation. They are fully opened to outside users for experiments using high brilliant synchrotron radiation from the undulator. The operation time of these beamlines are about 4000 hours and the number of users is more than 100 a year.

The staff members of SRL, the solid state spectroscopy group participate to the Materials Research Division of the Synchrotron Radiation Research Organization of the University of Tokyo (SRRO). They play essential roles in promoting scientific activities using SR and started to construct a new 25m-long undulator and beamline at the SPring-8, BL07-LSU. The beamline is equipped with experimental apparatuses using high brilliance synchrotron radi-



Fig. 1. The horizontal figure-8 undulators installed in SPring-8

ation in soft X-ray region. They are those for time-resolved experiments and nano-materials research experiments, which will only be possible using third generation light source and will promise us a considerable progress in the studies of nano-particles and real time observation of magnetic domains and of chemical reaction at catalytic surfaces, etc. They will be available in October in 2009.

The accelerator group performed the detailed design of the new 25-m undulator of the University of Tokyo in collaboration with the SPring-8 ID and accelerator groups. The four horizontal figure-8 undulator segments were already constructed and installed with a good alignment error in the long straight section of SPring-8. Field measurements of a phase shifter prototype started to be used in examining its performance. The accelerator group also studied future ERL (energy recovery linac) light sources and developed ERL components such as superconducting cavities and fiber laser oscillators for driving an ERL photocathode gun in collaboration with KEK, AIST and JAEA.

Neutron Science Laboratory

The Neutron Science Laboratory (NSL) has been playing a central role in neutron scattering activities in Japan since 1961 by performing its own research programs as well as providing a strong general user program for the university-owned various neutron scattering spectrometers installed at the JRR-3 operated by Japan Atomic Energy Agency in Tokai. In 2003, the Neutron Scattering Laboratory was reorganized as the Neutron Science Laboratory to further promote the neutron science with use of the instruments in JRR-3. Under the general user program supported by NSL, 14 university-group-owned spectrometers in the JRR-3 reactor (20MW) are available for a wide scope of researches on material science, and proposals close to 300 are submitted each year, and the number of visiting users under this program reaches over 6000 person-day/year.

Triple axis spectrometers and a high resolution powder diffractometer are utilized for a conventional solid state physics and a variety of research fields on hard-condensed matter, while in the field of soft-condensed matter science, researches are mostly carried out by using the small angle neutron scattering (SANS-U) and/or neutron spin echo (iNSE) instruments. The upgraded time-of-flight (TOF) inelastic scattering spectrometer is also available through the ISSP-NSL user program.

Major research topics on the hard-condensed matter science cover stripe order in high- T_c superconductors, and closely related 2 dimensional systems, charge and orbital



Fig. 1. The reactor hall of JRR-3. The eight neutron scattering instruments are attached to the horizontal beam tubes in the reactor experimental hall. Two thermal and three cold guides are extracted from the reactor core towards the guide hall located to the left.

ordering in CMR manganites, quadrupolar ordering in rare-earth based intermetallic compounds, spin dynamics of low dimensional dimmer systems, etc. On the other hand, the research topics on the soft-condensed matter science cover structural characterization of polymer gels, polymer blends, micelles, amphiphilic polymers, block copolymers, proteins, dynamics of brush-polymers on surface, slow dynamics of surfactants, pressure dependence of dynamics of amphiphilic membranes, and so on. In addition, there are a variety of activities on fundamental physics, neutron beam optics, developments of neutron scattering techniques.

The NSL also operates the U.S.-Japan cooperative program on neutron scattering, providing further research opportunities to material scientists who utilize the neutron scattering technique for their research interests.

The details of individual studies and research highlights in JFY2008 are reported in the NSL-ISSP Activity Report vol. 15. (http://quasi.issp.u-tokyo.ac.jp/actrep/actrep-15/index-pub_vol15.html).

Supercomputer Center

The Supercomputer Center (SCC) is a part of the Materials Design and Characterization Laboratory (MDCL) of ISSP. Its mission is to serve the whole community of computational condensed-matter physics of Japan providing it with high performance computing environment. In particular, the SCC selectively promotes and supports large-scale computations. For this purpose, the SCC invites proposals for supercomputer-aided research projects and hosts the Steering Committee, as mentioned below, to evaluate the proposals.

The SCC operates two super-computers, systems A and B. System A is Hitachi SR11000/48 that consists of 48 high performance nodes composed of tightly-coupled micro-processors. With the aid of the automatic parallelization of FORTRAN compiler, a node of System A can be used as if it were a single-processor computer. System A has 2.8TB memory and archives 5.8 TFlops peak performance in total. On the other hand, System B, which is SGI Altix 3700/1280,

is a parallel supercomputer with relatively loose coupling. It consists of 19 nodes inter-connected by a gigabit Ethernet network. Each node is a distributed-shared-memory-type computer consisting of 64 Intel Itanium 2 CPUs inter-connected by a rather high performance network and have 64 GB memory. System B archives 7.7 TFlops total throughput performance.

All staff member of university faculties or public research institutes in Japan are invited to propose research projects (called User Program). The proposals are evaluated by the Steering Committee of SCC. Pre-reviewing is done by the Supercomputer Project Advisory Committee. In school year 2008 totally 181 projects were approved. The total points applied and approved are listed on Table. 1 below.

The research projects are roughly classified into the following three (the number of projects approved):

- First-Principles Calculation of Materials Properties (67)
- Strongly Correlated Quantum Systems (40)
- Cooperative Phenomena in Complex, Macroscopic Systems (75)

All the three involve both methodology of computation and its applications. The results of the projects are reported in 'Activity Report 2008' of the SCC. Every year typically four projects are selected for "invited papers" and published at the beginning of the Activity Report. In the Activity Report 2008, the following four invited papers are included:

- "Vector spin chirality and multiferroic properties in one-dimensional spin-1/2 frustrated magnets", by Shunsuke FURUKAWA, Masahiro SATO, Yasuhiro SAIGA, and Shigeki ONODA
- "Jammed vortex matter" by Hajime YOSHINO, Tomoaki NOGAWA, Bongsoo KIM, and Hikaru KAWAMURA
- "Chemical reaction dynamics accompanying electron-transfer" by Osamu SUGINO

| Class | Max/Min Points | Application | Number of Projects | Total Points | | | |
|-------|----------------|--------------|--------------------|--------------|----------|----------|----------|
| | | | | Applied | | Approved | |
| | | | | System A | System B | System A | System B |
| A | <100K | any time | 2 | 150K | 50K | 150K | 50K |
| B | <2M | twice a year | 43 | 47M | 36M | 39M | 32M |
| C | <20M | twice a year | 127 | 1200M | 930M | 1046M | 851M |
| D | | any time | 9 | 175M | 155M | 173M | 145M |
| S | >20M | twice a year | 0 | 0M | 0M | 0M | 0M |
| Total | | | 181 | 1422M | 1121M | 1258M | 1028M |

Table 1. Research projects approved in 2008. The maximum points allotted to the project of each class are the sum of the points for the two systems; 1 K point of System-A corresponds to charge for 0.37 hours \times node, while the corresponding figure is 0.22 hours \times 64CPU for System-B.

International MegaGauss Science Laboratory

The aim of this laboratory is to study the physical properties of solid-state materials (such as semiconductors, magnetic materials, metals, insulators, superconducting materials) under ultra-high magnetic field conditions. Such a high magnetic field is also used for controlling the new material phase and functions. Our pulse magnets, at moment, can generate up to 85 Tesla by non-destructive manner, and from 100 up to 730 Tesla (the world strongest as an in-door record) by destructive (the single turn coil and the electro-magnetic flux compression) methods.

They are opened for scientists both from Japan and from overseas, especially from Asian countries, and many fruitful results are expected to come out not only from collaborative research but also from our in-house activities. One of our ultimate goals is to provide the scientific users as our joint research with magnets capable of a 100 T, milli-second pulses in a non-destructive mode, and to offer versatile physical precision measurements. The available measuring techniques now involve magneto-optical measurements, cyclotron resonance, spin resonance, magnetization and transport measurements.

Our interests cover the study on quantum phase transitions (QPT) induced by high magnetic fields. Field-induced QPT has been explored in various materials such as quantum spin systems, strongly correlated electron systems and other magnetic materials. Non-destructive strong pulse magnets are expected to provide us with reliable and precise solid state physics measurements. The number of collaborative groups for the research is over 50 in the year of 2007. Multiple extreme physical conditions combined with ultra-low temperatures and ultra-high pressures are also available.

A 210 MJ flywheel generator which is the world largest DC power supply (recorded in Guinness book of records in 1997/98) has been installed in the newly built DC Flywheel generator station at our Institute. The generator, once disas-



Fig. 1. The building for the flywheel generator (right hand side) and a long pulse magnet station (left hand side). The flywheel giant DC generator is 350 ton in weight and 5 m high (bottom). The generator, capable of a 51 mega watt out put power with a 210 mega joule energy storage, is planned to energize the long pulse magnet generating 100 Tesla without destruction.

sembled from the one used for Toroidal magnetic field coil in JFT-2M (JAERI Fusion Torus-2M) Tokamak nuclear fusion testing device, is now renewed as a power supply for the pulse magnets. The construction of the magnet service station has also been accomplished. The magnet technologies are intensively devoted to the quasi-steady long pulse magnet (an order of 1-10 sec) energized by the giant DC power supply, and also used for the outer-magnet coil to realize a 100 Tesla nondestructive magnet.

Our destructive magnets, such as the single-turn coil and the electro-magnetic flux compression (EMFC) systems, would be oriented toward easier access and more reliable measurements for solid-state physics than previously obtainable. One of our recent successes was the achievement of over 730 T within a 4 MJ energy injection by the EMFC, in which a new type of primary coil with a simpler design was employed. These are oriented for developing new horizons in material science realized under such extreme quantum limit conditions.

Enhancement of Optical Second Harmonic Generation by Nitrogen Adsorption on Cu(001)

G. Mizutani, N. Kawamura, and F. Komori

Optical second harmonic generation (SHG) is a powerful tool for investigating the electronic states of a solid system because it provides information both on occupied and unoccupied electronic states around the Fermi energy [1]. We have studied SHG from the clean and nitrogen (N) adsorbed Cu(001) surfaces. This system has attracted interest because on a partially N-covered Cu(001) surface a well ordered nano-grid pattern is formed from alternating clean and N-adsorbed surface areas [2]. The observed SHG signal was largely enhanced by the N adsorption. Surface SH responses of the Cu(001) surfaces based on electronic states were also studied using an *ab initio* approach, and the valence electronic states are compared with the results of angle resolved photoemission spectroscopy (ARPES).

Figure 1 shows the experimental results for the incident polarization angle dependence of the p- and s-polarized SHG intensity from the N-saturated, N-adsorbed grid, and clean Cu(001) surfaces. The p-polarized SHG intensity has a maximum for the p-polarized incident light for both the clean and N-adsorbed surfaces. The maximum values both on the N-saturated and N-adsorbed grid surfaces are 30 times larger than that on the clean surface. The s-polarized SHG intensity from the clean surface is a minimum for both the p- and s-polarized incident light. The calculated band structure for the N-saturated surface is consistent with the results of the ARPES measurement as shown in Fig. 2. The polarization angle dependence of SHG calculated for the same surface qualitatively agrees with the experimental observations, and the enhancement is mainly attributed to the change of the

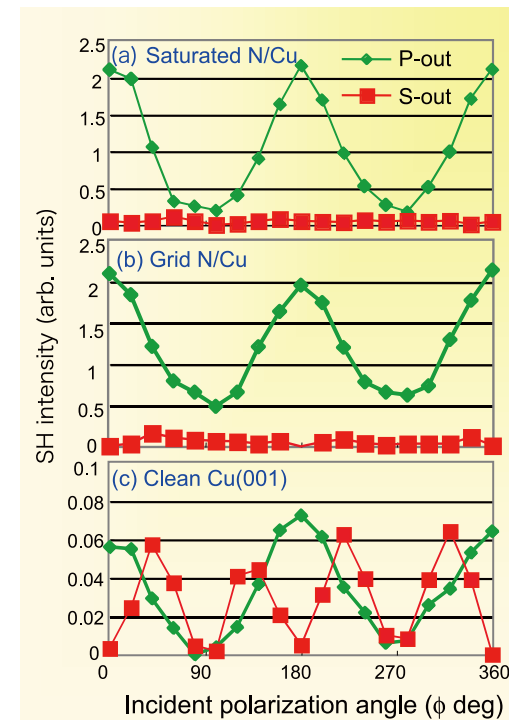


Fig. 1. Incident polarization angle dependence of the p- and s-polarized SHG intensity from the N-saturated (a), N-adsorbed grid (b), and clean (c) Cu(001) surfaces. The second harmonic light was generated by the incident light with a wavelength of 800 nm (1.55 eV). The origin of the incident polarization angle ($\theta = 0$) is p-polarized.

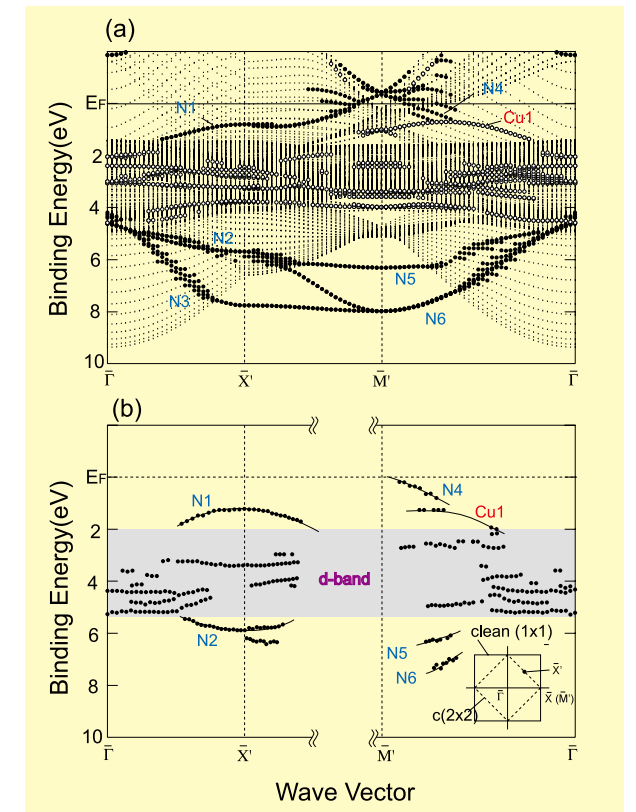


Fig. 2. (a) Calculated band structure of the Cu(001)c(2x2)-N surface along the Γ -X'-M'- Γ path. The filled circles indicate energy states of pronounced N 2p character, while the open circles correspond to states assignable to Cu atoms in the topmost and 2nd layer. (b) Experimentally observed N-derived states along the Γ -X' and Γ -M' directions by ARPES are plotted in the same energy and wave vector scale in Fig. 2(a). The gray zone is the d-band area. The inset shows the surface Brillouin zone of the clean and Cu(001)c(2x2)-N surfaces.

surface electronic states due to the N-adsorption.

On the grid surface, the p-SHG intensity generated by the p-polarized incident light is almost the same as that on the N-saturated surface. This is inconsistent with the simple assumption that the SHG signal originates from the N-covered c(2x2). The N-adsorbed area is 2/3 of the whole surface. Possible origins of the largely enhanced SHG on the grid surface are the lattice deformation due to the grid pattern formation and the presence of a long interface between the clean Cu surface and the N-adsorbed surface.

References

- [1] C. Schwaba, G. Meistera, A. Goldmann, and E. Bertel, *Surf. Sci.* **469**, 93 (2000).
- [2] F. M. Leibsle, C. F. J. Flipse, and A. W. Robinson, *Phys. Rev. B* **47**, 15865 (1993).

Authors

H. Sano^a, M. Miyaoka^b, T. Iimori, D. Sekiba, K. Nakatsuji, W. Wolf^c, R. Podloucky^d, N. Kawamura^b, G. Mizutani^a, and F. Komori^a
^aJapan Advanced Institute of Science and Technology
^bNHK Sci./Technical Research Laboratories
^cMaterials Design
^dUniversity of Vienna

Oxide Switch

I. Ohkubo and M. Lippmaa

Various oxide thin film-based switching devices have been proposed. Non-volatile switching between conducting

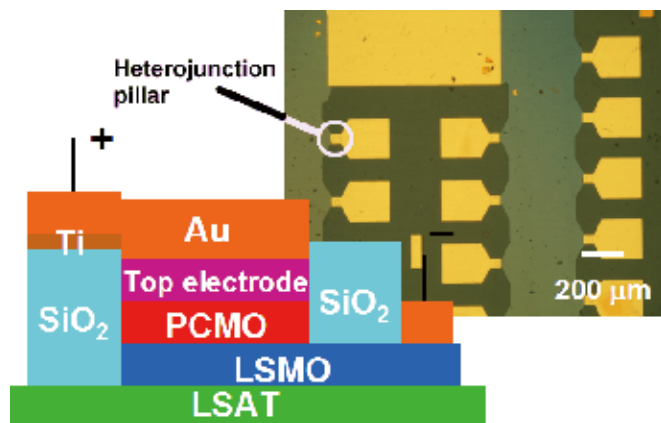


Fig. 1. Structure of the switching devices grown on $(\text{LaAlO}_3)_{0.3}\text{-(Sr}_2\text{AlTaO}_6)_{0.7}$ (LSAT) substrate. The bottom electrode is a metallic $(\text{La,Sr})\text{MnO}_3$ layer. Switching occurs either in the $\text{Pr}_{1-x}\text{Ca}_x\text{MnO}_3$ layer or at the top electrode interface. Vertical transport through the heterostructure occurs in micron-scale pillars that are etched into the thin film multilayer, shown in the inset photo.

and non-conducting states can occur under the influence of electric field, as in resistive switching, or by some other form of external excitation, such as light illumination or exposure to a magnetic field. In the present work, the purpose is to fabricate a trilayer oxide thin film device structure that can be used to measure transport in the perpendicular direction across a heterointerface as opposed to the more common planar geometry, in which transport is measured parallel to an active interface, *e.g.* in a field-effect transistor.

A cross-sectional schematic diagram and a plan-view photo of a lithographically patterned device are shown in Fig. 1. The thin film multilayer consisting of $(\text{La,Sr})\text{MnO}_3$ (LSMO) and $\text{Pr}_{1-x}\text{Ca}_x\text{MnO}_3$ (PCMO) is fabricated first by pulsed laser deposition, followed by a lithography step and ion milling that exposes and forms the shape of the LSMO bottom electrode. In the second step, the PCMO pillar structure is surrounded by a SiO_2 isolation layer and the device is finished by fabricating top metal electrodes by a lithographic lift-off process. Each sample contains several tens of pillar structures with diameters ranging from 5 to 50 μm .

Work is proceeding on characterizing the switching properties of these pillar samples. In case the top electrode is Aluminum, resistive switching occurs at the electrode / PCMO interface, driven by a field-induced formation of aluminum oxide at the top interface of the PCMO film.

Since the LSMO electrode and PCMO switching layers are both ferromagnetic oxides, it is also possible to study the magnetic properties of confined oxide microstructures and follow the transport properties of the magnetic heterostructures under external magnetic fields.

References

- [1] T. Harada *et al.*, Appl. Phys. Lett. **92**, 222113 (2008).
- [2] K. Tsubouchi *et al.*, Appl. Phys. Lett. **92**, 262109 (2008).
- [3] I. Ohkubo *et al.*, Mat. Sci. Eng. B **148**, 13 (2008).

Authors

I. Ohkubo^a, H. Kumigashira^{a,c}, M. Oshima^{a,c}, T. Ohnishi, K. Tsubouchi^a, Y. Matsumoto^b, K. Itaka^{a,c}, T. Harada^a, H. Koinuma^{a,c,d}, and M. Lippmaa^a
^aThe University of Tokyo
^bMaterials and Structures Laboratory, Tokyo Institute of Technology
^cCREST, Japan Science and Technology Corporation
^dNational Institute for Materials Science

Spin Waves, Vortex Excitations and Magnon BEC of Superfluid $^3\text{He-A}$ in Restricted Geometry, as in Parallel-Plates and in Oriented Aerogel

Y. Sasaki, O. Ishikawa, and M. Kubota

$^3\text{He-A}$ phase is a unique anisotropic superfluid state, composed with p-wave Cooper pairs of ^3He atoms. We present here recent two examples of our study, in which the orientation axis for \mathbf{d} vector, which represents the spin component of the Cooper pairs, is made perpendicular to \mathbf{l} vector, which represents the orbital angular momentum of the pair. The first example uses the sample placed between parallel plates with 12.5 μm gap, where we discuss a new observation of new satellite signal under rotation and possible half quantized vortices and Fréedericksz transition [1]. Whereas the second example uses Aerogel, a very dilute material with large open space of 98% volume, and with anisotropic orientation of the density gradient, to fill “ $^3\text{He-A}$ like” phase. We find macroscopic coherent precession of magnetization in this phase for the first time. This phenomenon is regarded as a manifest of the magnon Bose Einstein Condensation (BEC) in the magnetic superfluid $^3\text{He-A}$ [2].

Example 1: Quantized vortices with half-integer circulation, which are forbidden from existing in a conventional superfluid because of the single valuedness of the wave function, are theoretically predicted to exist in superfluid $^3\text{He-A}$ if the order parameters \mathbf{l} and \mathbf{d} form $\mathbf{l} \perp \mathbf{d}$ texture. To form the $\mathbf{l} \perp \mathbf{d}$ texture, we confined the superfluid $^3\text{He-A}$ between parallel plates with a 12.5 μm gap and applied a magnetic field of $H = 26.7$ mT perpendicular to the plates to take NMR and orient \mathbf{d} perpendicular to \mathbf{l} . NMR spectra exhibit a negative-shift peak which probes that the uniform $\mathbf{l} \perp \mathbf{d}$ texture is realized in our cell and show a new satellite signal under rotation. The rotation dependence of the satellite signal is interpreted that a Fréedericksz transition of \mathbf{l} texture is induced by rotation above 1.0 rad/s and vortices start to appear above 1.8 rad/s [1].

Figure 1 shows Rotation dependence of normalized size of the NMR satellite signal at 0.81 T_c , which indicates a transition, which we interpret as Fréedericksz transition, where uniform textural state transforms into a nonuniform

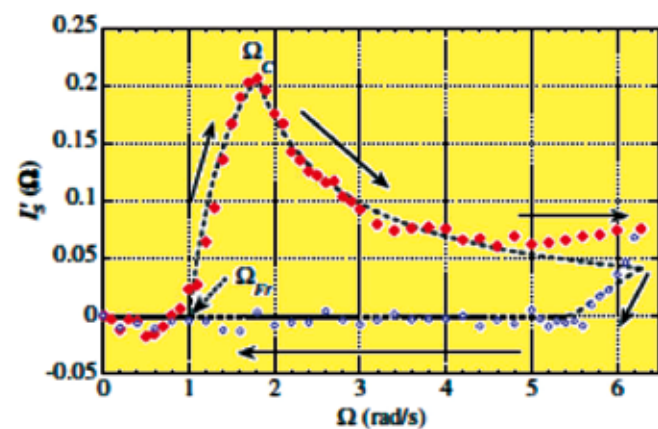


Fig. 1. Rotation dependence of normalized size of the NMR satellite signal at 0.81 T_c . Data taken in the acceleration (deceleration) process is shown in red filled (blue open) symbols. The dashed line is a model calculation based on the assumption that the Fréedericksz transition takes place for $\Omega \geq \Omega_{Fr}$ and vortices start to appear for $\Omega \geq \Omega_c$, where $\Omega_{Fr} = 1.0$ rad/s, $\Omega_c = 1.8$ rad/s. The peak at Ω_c changes its height as a function of T and seems to go to zero at T_c . An alternative explanation involving half quantized vortices is proposed[3] and further study is needed to clarify.

one. Actually, from this signal we analyze that singly or half quantized vortices start to penetrate into the sample from the edge at Ω_c . An alternative explanation has been proposed by H. Y. Kee and K. Maki[3], involving half quantum vortices.

Example 2: We report the first observation of coherent precession of magnetization in superfluid ^3He A-like phase (CPA) in aerogel [4]. The coherent precession in bulk ^3He A-phase is unstable due to the positive feed-back of spin supercurrent to the gradient of phase of precession. It was predicted that the homogeneous precession will be stable if the orbital momentum of the ^3He A-phase can be oriented along the magnetic field. We have succeeded to prepare this configuration by immersing uni-axially deformed anisotropic aerogel in ^3He . The dissipation rate of the coherent precession states in aerogel is much larger than that in bulk ^3He B-phase. We propose a mechanism of this dissipation. Actually this macroscopic coherent precession(MCP) is an evidence of BEC of magnons in $^3\text{He-A}$ as discussed in [5]. (The Coherent precession in $^3\text{He-A}$ is Partially reported in AR2007b).

References

- [1] M. Yamashita, K. Izumina, *et al.*, Phys. Rev. Lett. **101**, 025302 (2008).
- [2] T. Sato, T. Kunimatsu, K. Izumina, *et al.*, Phys. Rev. Lett. **101**, 055301 (2008).
- [3] H. Y. Kee and K. Maki, Europhys. Lett. **80**, 46003 (2007).
- [4] T. Kunimatsu, A. Matsubara, *et al.*, Physica C **468**, 605 (2008).
- [5] Yu. Bunkov and G. E. Volovik, Phys. Rev. Lett. **98**, 265302 (2007)

Authors

M. Yamashita^a, T. Sato, K. Izumina, A. Matsubara^b, Y. Sasaki^b, O. Ishikawa^c, T. Takagi^d, M. Kubota, T. Mizusaki^a, and Yu. M. Bunkov^e
^aKyoto University
^bResearch Center for Low Temperature and Materials Sciences, Kyoto University
^cOsaka City University
^dFukui University
^eMCBT, Institut Néel, CNRS/UJF

Pressure-Induced Superconductivity in Iron-Pnictide Materials

H. Okada, H. Takahashi, and Y. Uwatoko

High pressure studies have been playing a very important role for the investigations on the iron-pnictide superconductors, as well as carrier doping through substitution of atoms. In the earliest stage, applying pressure for optimally doped

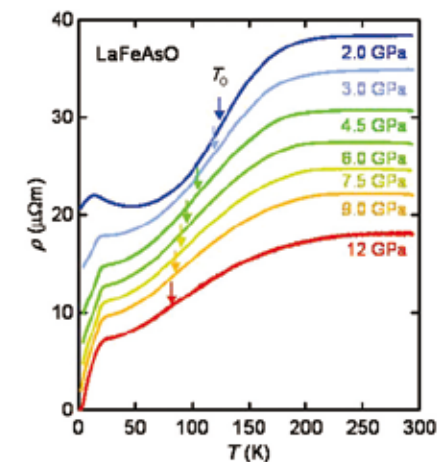


Fig. 1. ρ - T curves of LaFeAsO. The $d\rho/dT$ curve shows peak value at T_0 . At 12GPa, zero resistivity was observed.

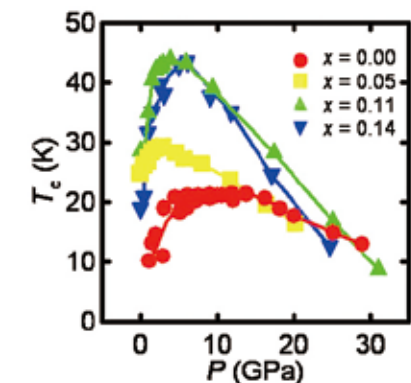


Fig. 2. Pressure dependence of the superconducting transition temperature in $\text{LaFeAsO}_{1-x}\text{F}_x$ series. The solid curves are guides to the eye.

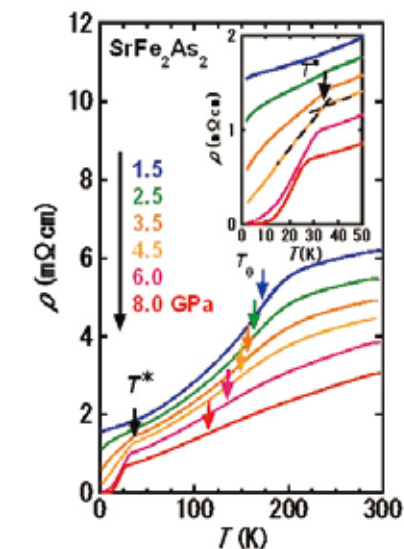


Fig. 3. ρ - T curves of SrFe_2As_2 . T_0 is defined as the same manner as LaFeAsO. At 8GPa, zero resistivity was observed.

$\text{LaFeAsO}_{1-x}\text{F}_x$ increased T_c to 43 K, which is the significantly large enhancement of T_c . Successive studies revealed the pressure-induced superconductivity for the undoped iron-pnictide materials [1].

Figure 1 shows the $\rho(T)$ curves of LaFeAsO using a cubic anvil press. The resistivity shows rapid decrease below 150 K, which is related to the structural and magnetic transitions (T_0). In the low temperature range, the sudden decrease of resistivity caused by superconductivity was observed. T_c increased up to 21 K at 12 GPa, where the zero resistivity was observed. This pressure-induced superconductivity was firstly discovered in the 1111 system. The T_0 , where the $d\rho/dT$ curve shows peak value, is suppressed by pressure, while T_c is enhanced with increasing pressure, as shown in Fig.2. The lightly doped and undoped $\text{LaFeAsO}_{1-x}\text{F}_x$ shows the comparatively lower maximum T_c than highly doped materials. This is thought that the lightly doped one is close to the magnetic phase. From the latest result on CaFeAsF , the pressure-induced superconductivity was observed above the pressure, where the T_0 was completely suppressed with pressure.

Figure 3 shows the $\rho(T)$ curves of SrFe_2As_2 using the cubic anvil press. Like as LaFeAsO, the T_0 was suppressed and superconductivity emerged under high pressure [2]. The zero resistivity was observed at 8GPa, which was the first observation for SrFe_2As_2 , although several pressure-induced superconductivity has been observed in AFe_2As_2 ($A = \text{Ca, Sr, Ba}$) system.

References

- [1] H.Okada *et al.*, JPSJ 77 113712 (2008).
 [2] K.Igawa *et al.*, JPSJ 78 025001 (2009).

Authors

H. Okada^a, H. Takahashi^a, K. Matsubayashi, and Y. Uwatoko^a
^aNihon University

Fabrication and Efficiency Evaluation of a Hybrid NiCrAl Pressure Cell up to 4 GPa

N. Fujiwara and Y. Uwatoko

Pressure has become increasingly important in the research on strongly correlated electron systems, because several 3d-transition-metal oxides, heavy fermion systems, and organic conducting systems exhibit a variety of phases with applied pressure. The phases include charge-ordering (CO), magnetic ordering, paramagnetic metallic, and superconducting (SC) states. In the case of pressure-induced superconductivity, a spin- or charge-ordering phase often appears at the lower pressure side on a pressure-temperature (P-T) phase diagram. Coexistence of the ordering states with the SC state, or anomalous metallic behavior near the quantum critical point (QCP), where the ordering state becomes unstable, is one of the current important topics in strongly correlated electron systems. In these compounds, some have been precisely investigated using various techniques under pressure, whereas the others have not. It is an important factor whether the onset pressure is achieved by a piston-cylinder-type pressure cell. The current borderline lies around a pressure of 2.7-3.0 GPa. Recently, NiCrAl or MP35N cylinders have attracted much attention as post-WC cylinders, because they are nonmagnetic and possess high tensile and yield strengths. In particular, NiCrAl contains fewer impurities than MP35N, and is suitable for magnetic measurements. In the present work, we applied loads up to 15.0 ton to a hybrid NiCrAl pressure cell and investigated the pressure limit and the efficiency.

We used a special press system arranged on the top flange of variable-temperature insert (VTI)(Fig. 1) [1]. The length between the top flange and the bottom of the VTI is 1340 mm. The pressure cell is screwed into the tension column made of MP35N, and the load is transferred to the

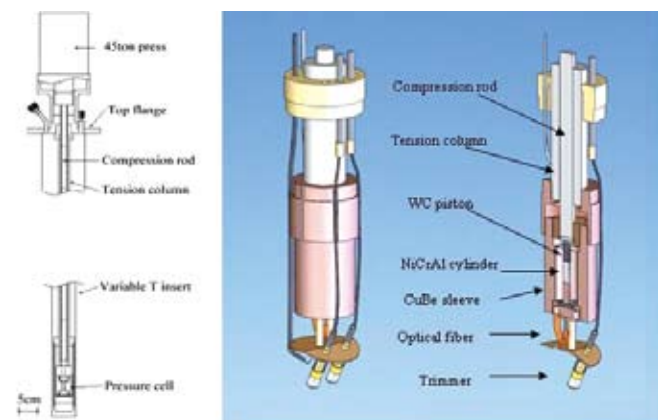


Fig. 1. Steady-load control system equipped on the top flange of variable-temperature insert (VTI). A load is transferred to the pressure cell via a compression rod. The pressure cell was screwed onto a tension column. The load is supported by the tension column, the CuBe sleeve and backup support. These components act as a frame of a conventional press system.

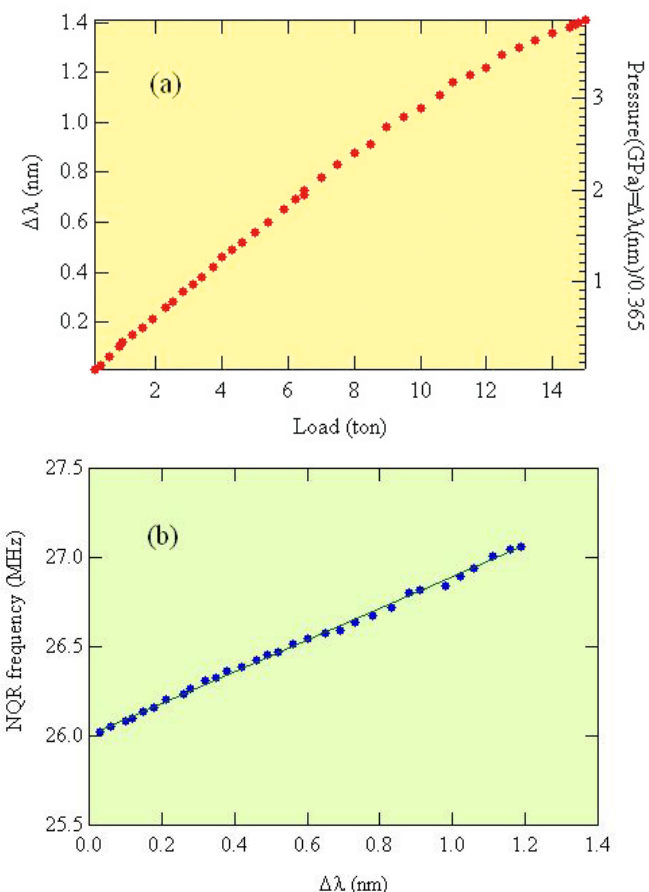


Fig. 2. (a) Load dependence of the R1 shift in ruby fluorescence. (b) Relationship between the NQR frequency of Cu₂O and the R1 shift.

pressure cell mediated by the inner compression rod. The tension column, the CuBe sleeve, and the CuBe backup support act as a frame in a conventional press system. Steady load control becomes possible owing to feedback from the pressure cell, even at low temperatures where pressure decrease is expected because of contraction of pressure mediation liquid. In the present VTI, two trimmer capacitors are equipped near the pressure cell to adjust NQR frequency and impedance matching. They are connected to tuning knobs outside the top flange by extension rods and can be controlled even at low temperatures.

⁶³Cu(I=3/2)-NQR measurement of Cu₂O and ruby fluorescence are very useful as means of pressure calibration because it does not require any sweeps of physical parameters. Ruby fluorescence is often adopted for diamond anvil cells. The shift of the R1 transition shows a linear relation with pressure. G. P. Piermarini, *et al.* measured pressure up to 19.5 GPa and obtained the fitting curve as $P(\text{GPa}) = \Delta\lambda/0.365$ (nm) [2]. Cu₂O is often used for pressure calibration in nuclear magnetic resonance (NMR) because the NQR frequency also shows a linear relation with applied pressure. We performed the ⁶³Cu NQR of Cu₂O and ruby fluorescence simultaneously using the steady-load control system mentioned above. Fig. 2 (a) shows load dependence of the R1 shift. As seen from the figure, the curve tends to bend downward with increasing load. The trend becomes remarkable when the heavy load is imposed. The bend is attributable to the loss of efficiency during the pressurizing process. Fig. 2(b) shows relationship between the NQR frequency and the R1 shift. We obtained the pressure dependence of the NQR frequency from Fig. 2(b) as $\nu(\text{MHz}) = 26.0 + 0.32P$ (GPa). The relation is consistent with an early study [3].

For the deformation of the cylinder during pressur-

izing process, the inner diameter partly expanded over 2% when a load of 15.0 ton was applied. The fracture strain of high-strength materials is usually not great, sometimes less than 3 %, therefore the upper pressure limit of the NiCrAl cylinder is at most 4 GPa. Furthermore, a crack was observed in the WC piston after releasing pressure from 4 GPa. The compression strength is 6 and 4.5 GPa for magnetic and nonmagnetic WCs, respectively. In the present experiment, we used the nonmagnetic WC, and therefore the appearance of the crack is not a surprising. To apply further pressure with this pressure cell, improvements to materials, especially for the piston, are also required as well as an effective sealing technique and the total design of the pressure cell.

References

- [1] N. Fujiwara, T. Matsumoto, K. Koyama-Nakazawa, A. Hisada, and Y. Uwatoko, Rev. Sci. Instrum. **78** 073905 (2007).
 [2] G. J. Piermarini, S. Block, J. D. Barnett, and R. A. Forman, J. App. Phys. **46** 2774 (1975).
 [3] A. P. Reyes, E. T. Ahrens, R. H. Heffner, P. C. Hammel, and J. D. Thompson, Rev. Sci. Instrum. **63** 3120 (1992).

Authors

N. Fujiwara^a, T. Matsumoto, K. Koyama-Nakazawa, A. Hisada^a, and Y. Uwatoko^a
^aKyoto University

Development of Electromagnetic Wave Absorber for Sub-terahertz Region in ϵ -type $\text{Al}_x\text{Fe}_{2-x}\text{O}_3$

M. Nakajima, S. Ohkoshi, and T. Suemoto

Recently, we have been studying the development of the electromagnetic wave absorber for millimeter wave in sub-terahertz range. This range is very expected for next-generation wireless communication. The development of the electromagnetic absorber in higher frequency region is urgent theme needed for the next-generation wireless communication. In general, when an electromagnetic wave is irradiated to a ferromagnet, the resonance due to gyromagnetic effect is caused. This resonance is called a “natural resonance” (ferromagnetic resonance) (Fig. 1). The resonance frequency (f_r) is proportional to a magnetocrystalline anisotropy field (H_a), which is expressed by $f_r = (\nu / 2\pi) H_a$, where ν is the gyromagnetic ratio. A magnetic material with a large coercive field (H_c) is expected to show a high-frequency resonance.

The sample $\epsilon\text{-Fe}_2\text{O}_3$ nanoparticles were prepared by an impregnation method based on mesoporous silica nanoparticles. The other samples for $x = 0.06, 0.09, 0.21, 0.30,$

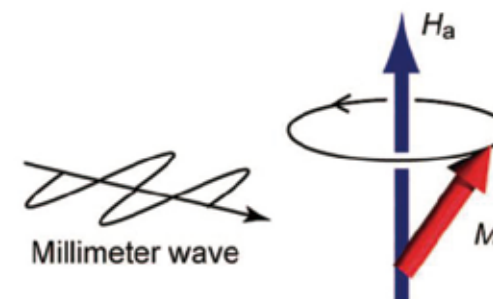


Fig. 1. Schematic illustration of the natural resonance due to the gyromagnetic effect. Precession of magnetization (M) around an anisotropy field (H_a) causes electromagnetic wave absorption.

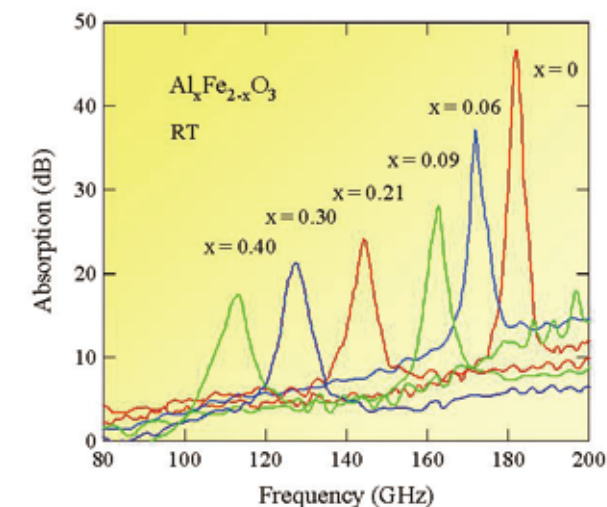


Fig. 2. The absorption spectra for $\epsilon\text{-Al}_x\text{Fe}_{2-x}\text{O}_3$ from $x = 0$ to 0.40 measured by THz time domain spectroscopy.

and 0.40 in $\epsilon\text{-Al}_x\text{Fe}_{2-x}\text{O}_3$ were prepared by a combination method between the reverse-micelle and sol-gel techniques. The average particle sizes of the materials are between 25 –50 nm. These nanomagnets have an extremely large H_c at 300 K of 10.2 kOe, 14.9 kOe, and 22.5 kOe for $x = 0.4, 0.21,$ and 0, respectively. In addition, aluminum is the third most common atom, the production cost is very economical, which is very attractive for practical applications.

Terahertz (THz) time domain spectroscopy using THz pulses emitted by femtosecond laser pulse excitation is powerful tool for investigating the millimeter wave and far-infrared region. The absorption measurement for $\epsilon\text{-Al}_x\text{Fe}_{2-x}\text{O}_3$ was performed at room temperature using by THz domain spectroscopy. As a THz wave emitter and detector, a dipole-type and bow-tie type low-temperature-grown GaAs photoconductive antennas were used, respectively. The absorption spectra of the THz waves were calculated by the following equation: (Absorption) = $-10 \log|t(\omega)|^2$ (dB) ($t(\omega)$; complex amplitude transmittance). An absorption of 20 dB indicates that 99 % of the introduced electromagnetic waves are absorbed, which is the target value for electromagnetic absorbers from an industrial point of view.

Figure 2 shows the absorption spectra. The frequencies of the absorption peaks for $x= 0.40, 0.30, 0.21, 0.09, 0.06,$ and 0 were observed at 112, 125, 145,162, 172, and 182 GHz, respectively (Fig. 2). In the case of a ferromagnetic material with a uniaxial magnetic anisotropy, the direction of magnetization was restricted around the magnetic easy-axis. When an electromagnetic wave is irradiated to a ferromagnetic material, the magnetization precesses around the easy-axis and a natural resonance occurs. The f_r value is proportional to the H_a . When the sample consists of randomly oriented magnetic particles, the H_a value is proportional to H_c . In fact, the f_r value increased as the H_c value increases.

High-performance millimeter wave absorbers composed of a series of $\epsilon\text{-Al}_x\text{Fe}_{2-x}\text{O}_3$ ($0 \leq x \leq 0.40$) nanomagnets were developed and investigated by the THz time domain spectroscopy. These magnetic materials exhibit natural resonances in the region of 112–182 GHz, which are the highest frequencies for magnetic materials. Such high natural resonance frequencies are achieved by the large magnetic anisotropies of this series.

Reference

[1] A. Namai, S. Sakurai, M. Nakajima, T. Suemoto, K. Matsumoto, M. Goto, S. Sasaki, and S. Ohkoshi, *J. Am. Chem. Soc.* **131**, 1170 (2009).

Authors

M. Nakajima, A. Namai^a, S. Sakurai^a, S. Ohkoshi^a, and T. Suemoto^a
^aThe University of Tokyo

Rashba Spin splitting of Surface States on Tl/Ge(111)-(3×1)

S. Hatta and T. Aruga

The spin splitting of two-dimensional (2D) electronic states due to the Rashba spin-orbit (SO) interaction is attracting much attention as a key to manipulate electron spins in solid state [1]. This type of spin splitting is caused by the out-of-plane asymmetry of the electronic potential. A surface makes such a potential asymmetry, and thus, intrinsic spin splitting is realized at surfaces. Sizable splittings exceeding ~0.1 eV have been observed on the surfaces of heavy elements such as Au and Bi. The potential of these high-Z nuclei contributes to a strong SO interaction. On the other hand, the observation of the giant Rashba splitting on Ag surfaces covered with submonolayer Bi [2, 3] indicates that the surface modification with heavy elements can enhance the spin splitting on surfaces of lighter elements, including semiconductors such as Si and Ge.

Here we report on the Rashba spin splitting of the Tl-induced surface state on the Ge(111) surface [4]. The Tl/Ge(111)-(31) surface has a quasi-one-dimensional structure, called “honeycomb-chain channel (HCC) structure”, with Ge adatoms of 4/3 monolayer (ML) and Tl of 1/3 ML. The HCC structure is commonly found for the other Si(111) and Ge(111) (3×1) surfaces with monovalent metals (alkali metals and Ag). These surfaces have similar electronic structures identified as the dangling bonds of the Si (Ge) adatoms. However, the spin splitting of these states has never been addressed. We found that the hybridization of the Tl and Ge orbitals induces large spin splittings on the surface states.

Figure 1 shows the calculated electronic structure of the (3×1) surface. Five surface-related states are found in the bulk band gap around the Fermi level. Using angle-resolved

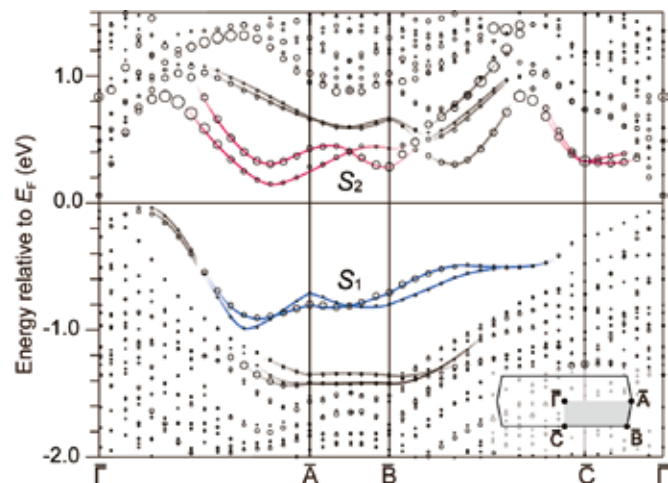


Fig. 1. Band structure of the Tl/Ge(111)-(3×1) surface calculated with the full-potential LAPW method. The radii of circles represent the contribution of the Tl 6p orbitals. The solid curves represent spin-split bands related to the Ge dangling bonds and Tl. The inset shows the (3×1) surface Brillouin zone.

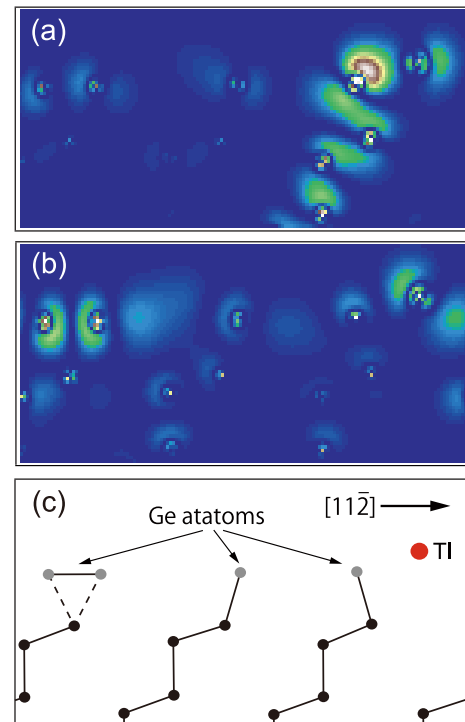


Fig. 2. Charge density plot of (a) S_1 and (b) S_2 at the A point. (c) Atomic structure of the Tl/Ge(111)-(3×1) surface.

photoelectron spectroscopy with synchrotron radiation at the ISSP beamline 18A of Photon Factory, we confirmed the corresponding occupied bands. These bands are split to pairs of spin-polarized bands respectively. Among them, large spin splittings of 0.1–0.2 eV are found for the S_1 and S_2 bands, indicated by the blue and red curves, respectively. The splittings are inhibited at the middle of Γ A and C. The spin degeneracy at the k points of $G/2$, where G represents the 2D reciprocal lattice vector, results from the coupling of the time-reversal symmetry and the translational symmetry. In the simple model with the 2D free electrons, the spin splitting shows a linear k dependence as $\Delta_R \propto 2\alpha_R k$, where α_R is called the Rashba parameter. However, the spin splitting on the (3×1) surface seems to become non-linear at k away from the proximity of the degeneracy points. This is partially due to the change of the orbital hybridization with k .

The orbital analysis of calculated states revealed that the largely spin-split states have a large contribution of the Tl 6p orbitals, as well as the Ge 4sp-hybridized orbitals. This is clearly shown in charge density plots of S_1 and S_2 at the A point (Fig. 2). The state of S_1 has a dominant dangling-bond character of the Ge adatom facing Tl. Moreover, the wavefunction of the spin-split state is spread over a few Ge layers. On the other hand, the charge distribution of S_2 is localized in the overlayer. Considering the charge density just around Tl, we found an asymmetry of the p -like distribution, reflecting the hybridization with 6s. According to an expression of $\alpha_R \propto \int d\mathbf{r} (\partial V/\partial z) |\psi(\mathbf{r})|^2$ [5], where V is the potential and $\psi(\mathbf{r})$ the wavefunction, while $(\partial V/\partial z)$ is approximately odd with respect to the nucleus, the asymmetric distribution of the wavefunction can lead to a large spin splitting collaborated with the nucleus potential, as observed on this surface. The hybridization of 6s-6p would be also important for the Rashba spin splitting of surface states induced by other heavy p -block elements such as Pb and Bi.

In conclusion, we have shown that the adsorption of submonolayer Tl induces the large Rashba spin splitting on Ge(111). The significant contribution of Tl 6p orbital is shown for the largely spin-split states.

References

[1] E. I. Rashba, *Sov. Phys. Sol. St.* **2**, 1109 (1960); Y. A. Bychkov, and E. I. Rashba, *JETP Lett.* **39**, 78 (1984).
 [2] T. Nakagawa, O. Ohgami, Y. Saito, H. Okuyama, M. Nishijima, and T. Aruga, *Phys. Rev. B* **75**, 155409 (2007).
 [3] C. R. Ast, J. Henk, A. Ernst, L. Moreschini, M. C. Falub, D. Pacilé, P. Bruno, K. Kern, and M. Grioni, *Phys. Rev. Lett.* **98**, 186807 (2007).
 [4] S. Hatta, T. Aruga, C. Kato, S. Takahashi, H. Okuyama, A. Harasawa, T. Okuda, and T. Kinoshita, *Phys. Rev. B* **77**, 245436 (2008).
 [5] M. Nagano, A. Kodama, T. ShiShidou, and T. Oguchi, *J. Phys.: Condens. Matter* **21**, 064239 (2009).

Authors

S. Hatta^a, T. Okuda^a, A. Harasawa, T. Kinoshita^{**}, and T. Aruga^a
^aKyoto University
^{*}current address: Hiroshima University
^{**}current address: JASRI/SPring-8

Quantum Phase Transition in the 3d Itinerant Antiferromagnet

H. Kadowaki and T. J. Sato

In recent years, novel viewpoints of matter have been exploited by quantum phase transitions (QPT), zero-temperature second-order phase transitions tuned by pressure or other controlling parameters. Around a QPT, the state of matter is characterized by singular behavior of fluctuating order parameters having both quantum mechanical and thermal origins. Quantum phase transitions are investigated in broad fields ranging from high temperature superconductors, metal-insulator transitions, to heavy fermions. Although a number of QPTs have been investigated experimentally and theoretically, many problems are under controversial debates. One of such debates is nature of QPT in itinerant antiferromagnets (AFM), referred to as the spin density wave (SDW) QPT. Experimentally, thermodynamic and transport properties are in rough agreement with theories of the SDW QPT. However, most neutron scattering studies seem to contradict expectations of the SDW QPT, exemplified by the novel E/T scaling of the AFM fluctuations observed in the heavy fermion $\text{CeCu}_{6-x}\text{Au}_x$, suggesting the existence of a new type of QPT [1]. In order to terminate the controversy, in this work we have performed neutron inelastic scattering

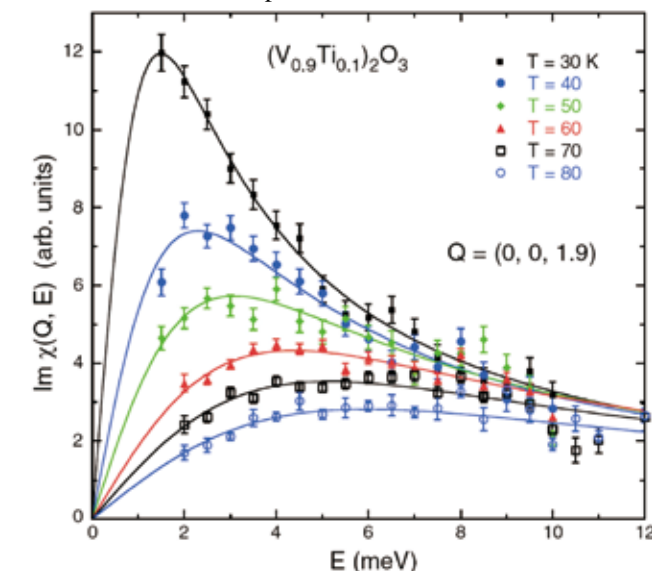


Fig. 1. Constant- Q scans measured at the AFM wave vector at several temperatures. Curves are fit results using Eq. (1). Error bars are statistical in origin and represent 1 standard deviation.

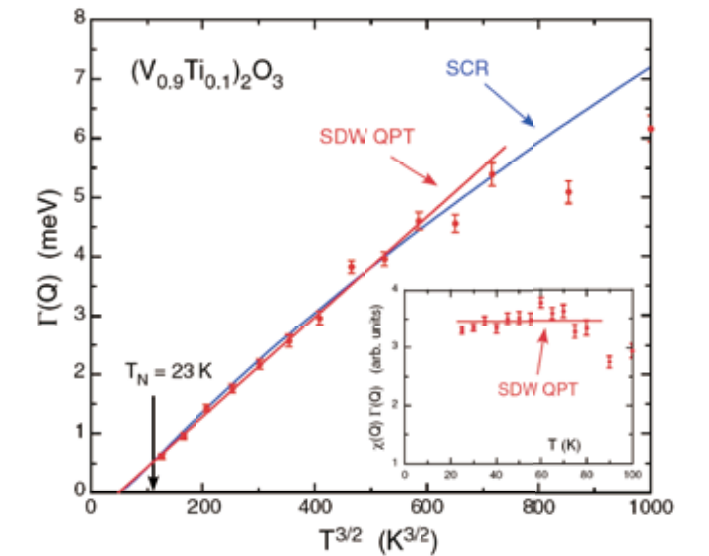


Fig. 2. Temperature dependence of the characteristic energy of the AFM spin fluctuations is plotted as a function of $T^{3/2}$. The curves represent the prediction for the SDW QPT and the fit using the SCR theory. The inset shows temperature dependence of the product $\chi(Q)\Gamma(Q)$.

study on the prototypical 3d itinerant antiferromagnet $(\text{V}_{1-x}\text{Ti}_x)_2\text{O}_3$ ($x = 0.1$), which is known to be in the proximity to the QPT separating paramagnetic and antiferromagnetic metal.

Figure 1 shows results of constant- Q scans at various temperatures in the paramagnetic region, which are converted to generalized susceptibility $\text{Im}\chi(Q, \hbar\omega)$. It was found that the generalized susceptibility is well approximated by the following Lorentzian function:

$\text{Im}\chi(Q+q, \hbar\omega) = \chi(Q)\Gamma(Q)\hbar\omega / \{ \hbar\omega^2 + [\Gamma(Q) + D(q_c^2 + Fq_{ab}^2)]^2 \}$, where Q is the AFM modulation vector, $\hbar\omega$ the excitation energy, q_c and q_{ab} components of q along c axis and in the ab plane. D and F are temperature independent parameters, whereas $\chi(Q)$ and $\Gamma(Q)$ are the wave-vector-dependent magnetic susceptibility and characteristic energy. Among several other predictions, the SDW QCP theory predicts temperature dependence of the characteristic energy as $\Gamma(Q) = c_1 + c_2 T^{3/2}$. To confirm this prediction, we have plotted the obtained $\Gamma(Q)$ parameters at various temperatures versus $T^{3/2}$ in Fig. 2. As seen in the figure, the $T^{3/2}$ behavior was confirmed up to $T = 80$ K. This concludes that QPT in this 3d itinerant antiferromagnet is governed by SDW QPT [2].

References

[1] S. Sachdev, *Quantum Phase Transitions* (Cambridge Univ. Press, Cambridge, 1999).
 [2] H. Kadowaki, K. Motoya, T. J. Sato, J. W. Lynn, J. A. Fernandez-Baca, and J. Kikuchi, *Phys. Rev. Lett.* **101**, 096406 (2008).

Authors

H. Kadowaki^a, K. Motoya^b, T. J. Sato, J. W. Lynn^c, J. A. Fernandez-Baca^d, and J. Kikuchi^e
^aTokyo Metropolitan University
^bTokyo University of Science
^cNIST Center for Neutron Research
^dOak Ridge National Laboratory
^eMeiji University

Quantum Phase Transition in Two-dimensional Antiferromagnets (CuCl)La(Nb_{1-x}Ta_x)₂O₇

H. Kageyama, Y. Ueda, and K. Kindo

Chimie douce offers rational design of the magnetic lattices in nonmolecular solids. For example, a new class of layered compounds (CuX)[A_{n-1}B_nO_{3n+1}] (where X = Cl⁻, Br⁻, A = La³⁺, Ca²⁺, Na⁺..., B = Nb⁵⁺, Ta⁵⁺, Ti⁴⁺..., n = 2, 3) has been obtained by low-temperature ion-exchange reactions [1-6]. As shown in Fig. 1(a), the magnetic CuX layer is separated well by magnetically inert A_{n-1}B_nO_{3n+1} perovskite slabs, making them good two-dimensional spin-1/2 magnets. Several exotic quantum magnetic phenomena have been observed such as collective singlet-ground states in (CuCl)LaNb₂O₇, collinear order at 32 K in (CuBr)LaNb₂O₇, 1/3 magnetization plateau in (CuBr)Sr₂Nb₃O₁₀.

In order to obtain the origin of the spin-singlet formation in (CuCl)LaNb₂O₇, we investigated the magnetic properties of (CuCl)La(Nb_{1-x}Ta_x)₂O₇ by means of transmission electron microscopy (TEM), susceptibility, pulsed high-field magnetization, and elastic/inelastic neutron scattering [7]. A crucial advantage of studying this solid solution is that the magnetic CuCl plane is preserved and that pentavalent Nb and Ta ions have almost the same radius (0.64 Å).

The X-ray diffraction patterns of the 0 < x < 1 samples showed designed synthesis of the solid solution having nearly the same tetragonal cell parameters as those of (CuCl)LaNb₂O₇ and (CuCl)LaTa₂O₇. The TEM experiments for (CuCl)LaNb₂O₇ carried out typically at room temperature using a JEM2010F system with an operating voltage of 200 kV revealed weak reflections such as (1/2, 0, 0) and (0, 1/2, 0). This indicates the doubling of the a- and b-axis [6]. Similar patterns are also obtained for the solid solution. A uniform distribution of the Nb and Ta atoms is confirmed by the energy-dispersive spectroscopy (EDS) spectrum as shown in Figs. 1 (c), (d).

From the magnetization curves (Fig. 2), it is seen that the spin-singlet state is stable up to x ~ 0.4, accompanied by a slight reduction of the spin gap with increasing x. On the

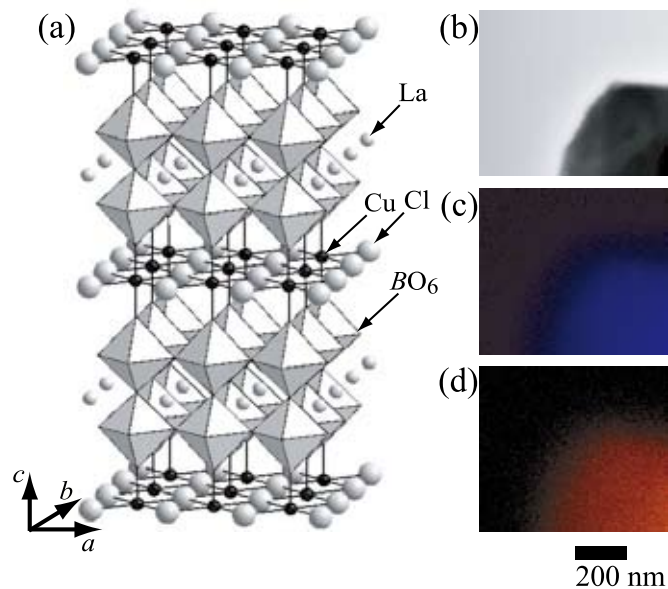


Fig. 1. (a) Schematic view of the crystal structure of (CuCl)LaB₂O₇ (B = Nb, Ta). (b) TEM image and (c), (d) the corresponding EDS maps of the x = 0.8 sample, where blue and red dots represent Nb and Ta, respectively.

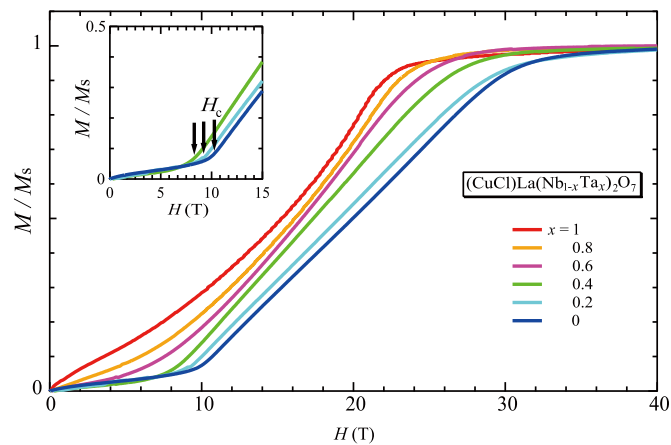


Fig. 2. Magnetization curves M of (CuCl)La(Nb_{1-x}Ta_x)₂O₇ at $T = 1.3$ K. Inset is an enlarged plot for $x = 0, 0.2$ and 0.4 , highlighting the critical fields H_c .

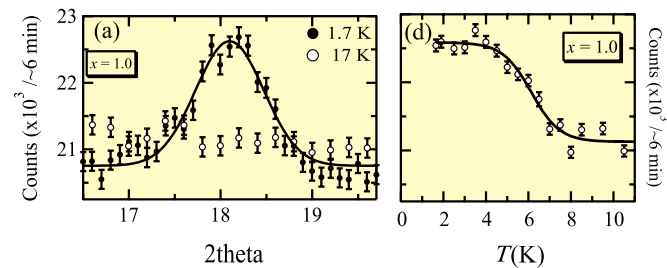


Fig. 3. Neutron diffraction profiles of $x = 1$ around the $(\frac{1}{2}, 0, \frac{1}{2})$ magnetic reflection. Open and closed circles represent the data collected at 1.7 and 17 K, respectively, and the solid line is a guide to the eye.

other hand, the neutron diffraction study (Fig. 3) revealed that (CuCl)LaTa₂O₇ undergoes, in spite of unaltered cell parameters and preserved CuCl plane, collinear order with $T_N \sim 7$ K. In the intermediate region (0.4 < x < 1), we observed the collinear order with a significantly reduced magnetic moment but with a nearly constant T_N , suggesting that the collinear order state coexists with the spin-singlet state.

References

- [1] H. Kageyama, T. Kitano, N. Oba, M. Nishi, K. Hirota, L. Viciu, J. B. Wiley, J. Yasuda, Y. Ajiro, and K. Yoshimura, *J. Phys. Soc. Jpn.* **74**, 1702 (2005).
- [2] H. Kageyama, J. Yasuda, T. Kitano, K. Totsuka, Y. Narumi, M. Hagiwara, K. Kindo, Y. Baba, N. Oba, Y. Ajiro, and K. Yoshimura, *J. Phys. Soc. Jpn.* **74**, 3155 (2005).
- [3] A. Kitada, Z. Hiroi, Y. Tsujimoto, T. Kitano, H. Kageyama, Y. Ajiro, and K. Yoshimura, *J. Phys. Soc. Jpn.* **76**, 093706 (2007).
- [4] N. Oba, H. Kageyama, T. Kitano, J. Yasuda, Y. Baba, M. Nishi, K. Hirota, Y. Narumi, M. Hagiwara, K. Kindo, T. Saito, Y. Ajiro, and K. Yoshimura, *J. Phys. Soc. Jpn.* **75**, 113601 (2006).
- [5] Y. Tsujimoto, Y. Baba, N. Oba, H. Kageyama, T. Fukui, Y. Narumi, K. Kindo, T. Saito, M. Takano, Y. Ajiro, and K. Yoshimura, *J. Phys. Soc. Jpn.* **76**, 063711 (2007).
- [6] M. Yoshida, N. Ogata, M. Takigawa, J. Yamaura, M. Ichihara, T. Kitano, and H. Kageyama, *J. Phys. Soc. Jpn.* **76**, 104703 (2007).
- [7] A. Kitada *et al.*, submitted to *Phys. Rev. B*.

Authors

H. Kageyama^a, Y. Ajiro^a, K. Yoshimura^a, M. Nishi, Y. Narumi, K. Kindo, M. Ichihara, and Y. Ueda
^aKyoto University

Jammed Vortex Matter

H. Yoshino and T. Nogawa

Irrationally frustrated Josephson junction array (JJA), namely JJA with irrational number density of vortices per plaquette induced by external magnetic field, is a highly frustrated system which refuses to be stabilized in simple periodic manners [1]. The irrationally JJA with spatially *isotropic* Josephson coupling on the square lattice is believed to remain in a vortex liquid state down to zero temperature [2]. However we found strong numerical evidences obtained by extensive Monte Carlo simulations for static properties and RCSJ (Resistively and Capacitively Shunted Junction) simulations for transport properties [3], that even an *infinitesimally weak anisotropy* of the Josephson coupling into, say x and y directions induce formation of smectic layers of zigzag vortex stripes. (Fig. 1)

The vortex pattern is essentially frozen in random zigzag patterns but the whole frozen-structure can slide into the direction of stronger coupling due to phason like gapless soft modes. Consequently the system behaves as an unusually fragile matter [3]: solid like (non-Ohmic, superconducting) response against external shear on the phase variables (injection of the external electric current) perpendicular to the layers but liquid like (Ohmic) response against shear parallel to the layers. By the same token, the superconducting phase coherence remains disordered down to zero temperature, which is analogous to the spin-chirality decoupling phenomena observed in frustrated magnets [4].

Our motivation to study the anisotropic JJA originates from an unexpected connection to a class of friction models which exhibit the so called Aubry's transition [5] which is a prototype of jamming transition [6]. We found the current vs voltage curves exhibit scaling properties similar to those of the flow curves (shear-stress vs shear-rate) studied in the non-linear rheology of granular materials around jamming point [7]. In the Fig. 2 we summarize our results by showing the phase diagram of the system. Apparently it is very similar to the one proposed for the rheology of granular and soft-glassy systems [6,7].

In Addition to the JJA, we also studied the transport (rheological) properties of the semi-elastic model in which the sinusoidal coupling in the original JJA model into one

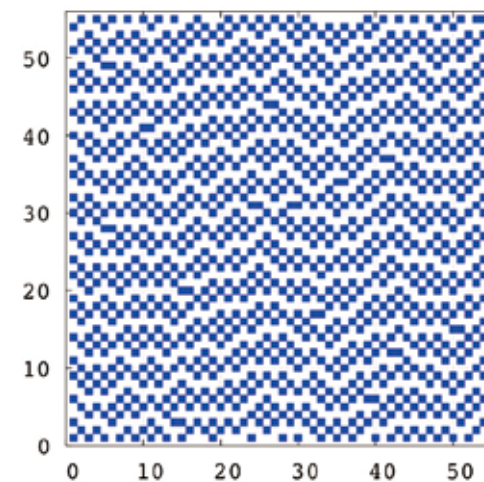


Fig. 1. Smectic zigzag vortex pattern of the irrationally frustrated anisotropic JJA in equilibrium. The blue/white boxes represent presence/absence of vortices in the plaquette of the JJA. In this example Josephson coupling is 1.5 times stronger into the vertical direction than to the horizontal direction.

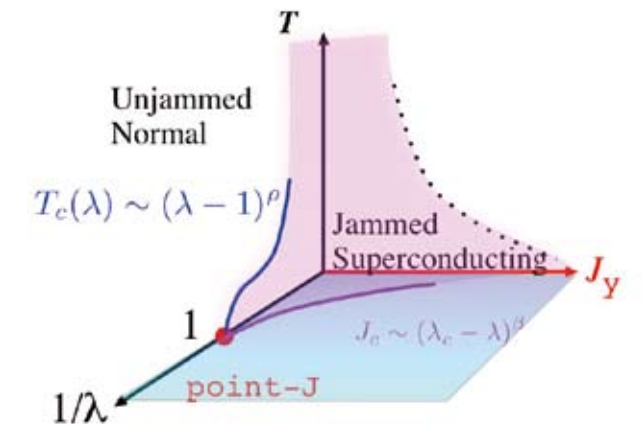


Fig. 2. "Jamming phase diagram" of the irrationally frustrated anisotropic JJA.

direction is replaced by an elastic coupling. The latter model is presumably closer to the friction model [5]. Indeed we found the scaling function of the current-voltage curve of the semi-elastic model is almost indistinguishable from the master flow-curve observed in granular systems [7]. Further investigations to clarify relationships among the JJA, semi-elastic model and the 1-dim friction models [5] will be certainly rewarding.

Whether geometrical frustration alone can realize glassy phases is a long-standing issue. Halsey [1] has envisioned that the irrationally frustrated JJA can exhibit a glassy phase. Our observations suggest the *anisotropic* irrationally frustrated JJA realizes *floating zigzag stripe glass states*. The intriguing question is whether these 'states' constitute real thermodynamic glass states. We plan to perform further investigation to give a definitive answer to this fundamental question.

References

- [1] T. C. Halsey, *Phys. Rev. Lett.* **55**, 1018 (1985).
- [2] E. Granato, *Phys. Rev. Lett.* **101**, 027004 (2008).
- [3] H. Yoshino, T. Nogawa, and B. Kim, *New J. Phys.* **11**, 013010 (2009). Movies of the transport dynamics are available in "Supplementary Data" at <http://iopscience.iop.org/1367-2630/11/1/013010/>
- [4] S. Teitel and C. Jayaprakash, *Phys. Rev. B* **27**, 598 (1983); H. Kawamura and M. Tanemura, *Phys. Rev. B* **36**, 7177 (1987).
- [5] M. Peyard and S. Aubry, *J. Phys. C: Solid State Phys.* **16**, 1593 (1983); H. Matsukawa and H. Fukuyama, *Phys. Rev. B* **49**, 17286 (1994).
- [6] *Jamming and Rheology*, Ed. A. J. Liu, S. R. Nagel, CRC Press (2001).
- [7] P. Olsson and S. Teitel, *Phys. Rev. Lett.* **69**, 178001 (2007); T. Hatano, *J. Phys. Soc. Jpn.* **77**, 123002 (2008); M. Otsuki and H. Hayakawa, *Prog. Theor. Phys.* **121**, 647 (2009).

Authors

H. Yoshino^a, T. Nogawa^b, B. Kim^c, and H. Kawamura^a
^aOsaka University
^bThe University of Tokyo
^cChangwon University

Evidence of Spin Singlet Ground State in the Frustrated Antiferromagnetic Ring Cr₈Ni

Y. Furukawa, Y. Narumi, and K. Kindo

Recently there has been intense experimental and theoretical effort in synthesis and investigation of nanoscale molecular magnetic systems, which are composed of a controllable number of transition metal ions [1]. The discovery of

quantum phenomena [2,3] like quantum tunneling of the magnetization observed in single molecule magnets has further increased the interest in the investigation of nanoscale molecular magnets. Among nanoscale molecular magnets are antiferromagnetic (AF) rings that have an almost coplanar ring shape with a number (N) of transition metal ions. A common feature of all even number rings is to have a spin singlet $S_T = 0$ ground state due to the dominant AF Heisenberg exchange couplings between nearest neighbor spins. Due to the finite size effects, AF rings have a discrete energy spectrum and the lowest-lying magnetic excited states [4].

In the case of odd-number AF rings, magnetic properties are expected to be changed drastically due to spin frustration. The simplest systems of odd-number molecular AF rings are the $s = 1/2$ three spin system with an AF interaction. In these frustrated triangular AF spin systems the ground state is a magnetic $S_T = 1/2$ state [5]. Odd number AF rings with $N > 3$ have been more difficult to synthesize. Quite recently a breakthrough in the synthesis of a new family of odd-number AF rings with $N=9$ was achieved. A heterometallic Cr-based ring-shaped AF magnet ($C_2H_{11}N_2NH_2\{Cr_8NiF_9[O_2CC(CH_3)_3]_{18}\}$ (abbreviated as, Cr_8Ni) was synthesized [6]. As a matter of fact, Cr_8Ni is the first odd-member AF ring with $N > 3$. This system has spin frustration effects because all AF interactions cannot be simultaneously satisfied.

The schematic structure of the core of Cr_8Ni is shown in Fig. 1(a). The metal ions are bridged by one fluorine ion and two $(CH_3)_3CCO_2$ radicals [6]. The AF interactions between the Cr ions and between the Cr and the Ni ions are reported to be $J_{Cr-Cr}=16K$ and $J_{Cr-Ni}=70K$, respectively, from the fit of the temperature dependence of magnetic susceptibility χ which shows peaks around 2 K and 25 K (see Fig. 1(b)) [6]. From the fitting of the magnetic susceptibility in the temperature range $T = 1.6-300$ K it is also inferred that the ground state is a singlet $S_T = 0$ and that the first excited state is a $S_T = 1$ state at 3.7 K from the ground state. The fit was based on a spin Hamiltonian that included Heisenberg exchange terms only [6]. The conclusion about the singlet ground state in

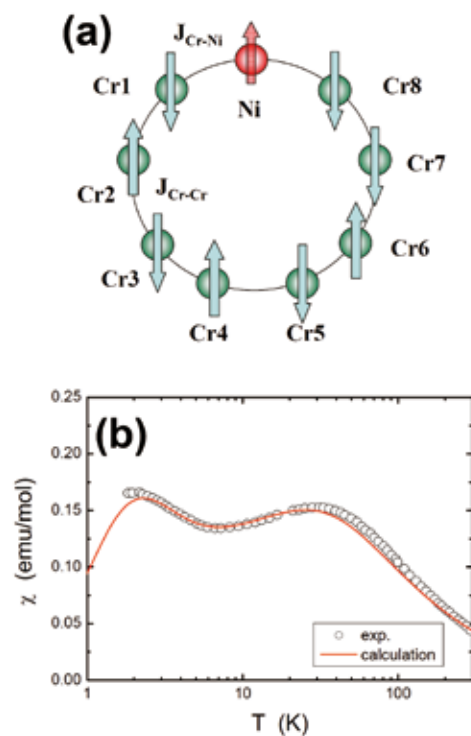


Fig. 1. (a) Schematic view of Cr_8Ni . (b) Temperature dependence of magnetic susceptibility of Cr_8Ni from ref. 6. The solid line shows the theoretical calculated results.

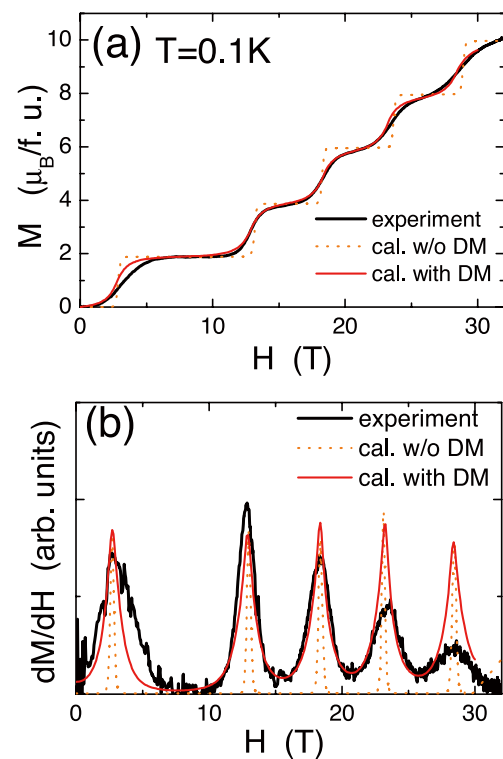


Fig. 2. (a) Magnetization curve of Cr_8Ni measured at $T = 0.1$ K (black solid line). Red lines show the theoretical calculated results (dotted line; without DM interaction, solid line; with DM interaction). (b) dM/dH curve at $T = 0.1$ K. Red lines show the theoretical calculated results (dotted line; without DM interaction, solid line; with DM interaction).

this frustrated ring is quite novel and interesting and it thus requires more direct experimental evidence. In order to elucidate the ground state of the Cr_8Ni system from experimental point of view, it is important to investigate the magnetic properties at much lower temperature i.e. well below the lowest energy gap. For the purpose, we have carried out high field magnetization measurements at very low temperatures down to 0.1 K.

Figure 2(a) shows the magnetization (M) curves for Cr_8Ni at $T = 0.1$ K for increasing magnetic fields, where a clear step-wise increase of magnetization is observed. Our experimental results clearly show an evidence of a spin singlet ground state for the Cr_8Ni system and allow us to establish the energy separation of the low-lying quantum magnetic states. The experimental results are in good agreement with predictions from theoretical calculations. Interestingly, the width of the steps in the field-dependence of the magnetization show that sizeable Dzyaloshinski-Moriya (DM) interactions are present and lead to anticrossings between states of different total spin.

References

- [1] D. Gatteschi *et al.*, "Molecular Nanomagnets" (Oxford University Press, 2006).
- [2] L. Thomas *et al.*, Nature **383**, 145 (1996).
- [3] C. Sangregorio *et al.*, Phys. Rev. Letters **78**, 4645 (1997).
- [4] J. Schnack and M. Luban, Phys. Rev. B **63**, 014418 (2000).
- [5] D. Gatteschi *et al.*, Nature (London) **354**, 463 (1991).
- [6] O. Cador *et al.*, Angew. Chem. Int. Ed. **43**, 5196 (2004).

Authors

Y. Furukawa^a, K. Kumagai^b, Y. Ajiro^c, Y. Narumi^d, K. Kindo, P. Santini^e, F. Borsa^f, R. E. P. Winpenny^g
^aIowa State University
^bHokkaido University
^cKyoto University
^dIMR, Tohoku University
^eUniversita di Parma
^fUniversita di Pavia
^gUniversity of Manchester

Field-Induced Magnetic Phase Transitions in Multiferroic $RbCoBr_3$.

M. Tokunaga and Y. Nishiwaki

Recently, emergence of direct coupling between magnetism and electric polarization in ferroelectric magnets has attracted considerable attention in condensed-matter physics. Since magnetic moment (M) and electric polarization (P) have different parity for time-reversal and spatial-inversion operation, linear combination between the both order parameters usually does not contribute to the free energy. Strong coupling between the both is put into reality when some kinds of spatially modulated spin structures set in. As a typical example, magnets with cycloidal spin states have been the most extensively studied, in which the accompanying P is caused by the anti-symmetric exchange interaction between the adjacent spins [1,2]. On the other hand, another multiferroic state in which symmetric exchange interaction plays the essential role is less understood although theoretical calculation predicts the presence of the larger P in this mechanism [3].

In this context, we brought our attention to a frustrated Ising magnet of $RbCoBr_3$. In this material, spins in the Co^{2+} ions construct quasi-one-dimensional antiferromagnetic chains along the c -axis. The chains form a triangular lattice within the ab -plane (see inset of Fig. 1) having antiferromagnetic nearest neighbor interaction. As a consequence of this frustration, successive magnetic transitions, i.e. from partial disorder to ferrimagnetic states, take place with decreasing temperature [4]. Dielectric measurement revealed that these magnetic transitions are accompanied with a significant change in P [5]. Due to the strong Ising-type anisotropy, this

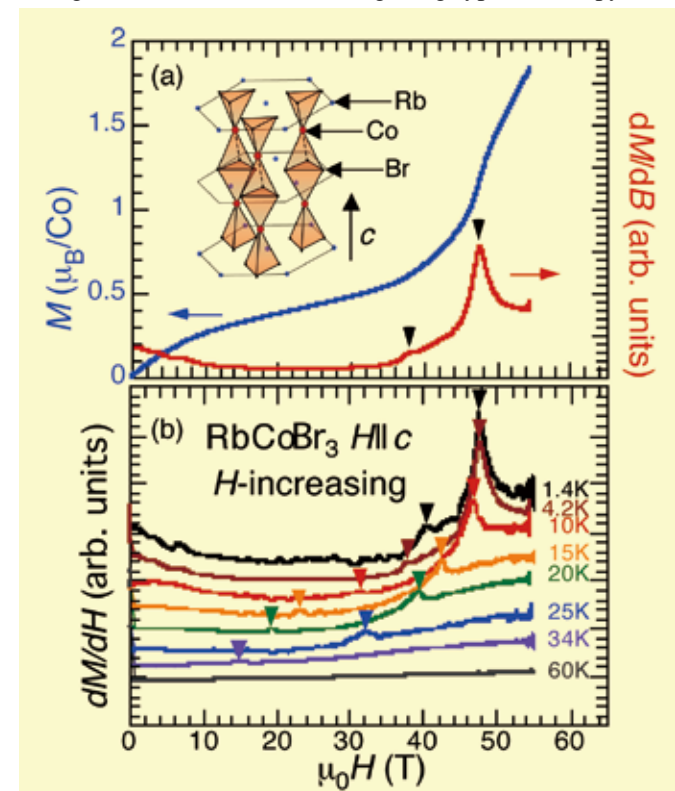


Fig. 1. (a) A Magnetization curve (blue) and differential susceptibility (red) of $RbCoBr_3$ at 4.2 K in a pulsed magnetic field of 55 T applied along the c -axis. We assigned two anomalies in the differential susceptibility as marked by the triangles. Crystallographic structure of the $RbCoBr_3$ is schematically drawn in the inset. (b) Field dependence of the differential susceptibilities in the field-increasing process at various temperatures. The plot for each temperature was offset for clarity.

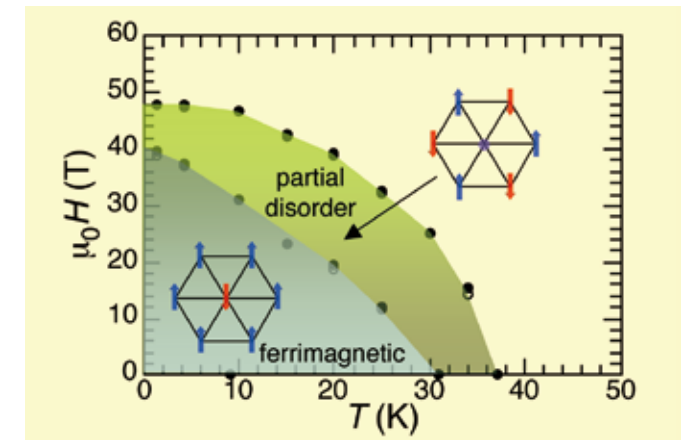


Fig. 2. Magnetic phase diagram of $RbCoBr_3$ for $H \parallel c$ -axis. The schematic drawing in the inset demonstrate the possible spin structure within the ab -plane in each phase.

material shows collinear spin ordering, and hence, antisymmetric-type mechanism cannot account for the emergence of the P . In this study, we studied isothermal magnetization curves up to 55 T to clarify whether external magnetic fields (H) can modify the spin state that couples with ferroelectricity in this material.

Figure 1(a) shows magnetization curve (blue) and differential susceptibility (dM/dH ; red) of $RbCoBr_3$ in $H \parallel c$ -axis at 4.2 K. In addition to a steep increase in M at around 48 T, small change in the slope (cusp in the dM/dH) is discernible at around 38 T as marked by the triangles. The presence of these anomalies is confirmed by taking systematic temperature variation of the dM/dH curves. As shown in Fig. 1(b), the both anomalies shift to the lower fields as temperature increases. Temperature dependence of the cusp field is demonstrated in Fig. 2. The both anomalies smoothly approach the magnetic transition temperatures in zero field. Thus we derive the phase diagram as described in Fig. 2: the ferrimagnetic state at the ground state changes into partial disorder phase by application of H . Presence of successive magnetic transitions implies the accompanying change in P . Further studies on electric polarization are in progress.

References

- [1] H. Katsura, N. Nagaosa, and A. V. Balatsky, Phys. Rev. Lett. **95**, 057205 (2005).
- [2] M. Mostovoy, Phys. Rev. Lett. **96**, 067601 (2006).
- [3] I. A. Sergienko and E. Dagotto, Phys. Rev. B **73**, 094434 (2006).
- [4] Y. Nishiwaki, T. Nakamura, A. Oosawa, K. Kakurai, N. Todoroki, N. Igawa, Y. Ishii, and T. Kato, J. Phys. Soc. Jpn. **77**, 104703 (2008).
- [5] K. Morishita, T. Kato, K. Iio, T. Mitsui, M. Nasui, T. Tojo, and T. Atake, Ferroelectrics **238**, 105 (2000).

Authors

M. Tokunaga and Y. Nishiwaki^a
^aTokyo Women's Medical University

International Conferences and Workshops

Topological Aspects of Solid State Physics

June 2-22, 2008
M. Kohmoto and M. Oshikawa

As the third in the series of International Workshops organized by ISSP theory group, "Topological Aspects of Solid State Physics" (TASSP) was held for the first three weeks of June 2008 at ISSP. In the following week (June 23 – June 27), a Symposium with the same title was held at Yukawa Institute for Theoretical Physics (YITP), Kyoto University. The Workshop part and the Symposium part were sponsored by ISSP and YITP, respectively. Both parts were also sponsored by Institute for Complex Adaptive Matter (ICAM-I2CAM) with U.S. NSF Grant DMR-064546. The number of registered participants in the entire period was 110 (72 in the Workshop at ISSP), including 26 invited participants (17 in the Workshop at ISSP) from overseas. In this report, we mostly focus on the activities in the Workshop at ISSP, which was co-chaired by Mahito Kohmoto and Masaki Oshikawa of ISSP with support from many people inside and outside ISSP.

Application of topological notion to condensed matter physics started several decades ago. One of the most notable examples is quantum Hall effect, where the quantization of a physical quantity (Hall conductance) may be understood in terms of topological invariant (Chern number). Recently, more variety of systems is found to exhibit exotic quantum behaviors, and ideas based on topology appear to be essential in understanding them. These include spin quantum Hall effect, graphenes, topological phases of quantum spin systems. While each of these subjects is certainly worth individual attention, the purpose of this Workshop was to cultivate unified understanding of those diverse phenomena, based on topological concepts.

Reflecting the concept of the Workshop, there was a wide range of subjects of talks. While the Workshop is largely oriented for theorists, three talks were given by experimentalists at ISSP to discuss their recent results from the topological perspective. There were 22 talks during the three weeks of Workshop at ISSP, and on average there were more than 20 people in the audience for each talk.

The main aim of the Workshop was to encourage informal discussions and collaborations. In order to serve the purpose, at most only two talks were scheduled each day to leave ample time for discussion. This format was well received by the participants, and in fact we could always hear lively discussion during the free time. As an outcome, several publications based on collaborations initiated at the Workshop have been already reported.

The program and other details of the Workshop, including videos of the talks, can be found at the Workshop web page URL <http://www.issp.u-tokyo.ac.jp/public/TASSP/index.html>

International Spring School on "Sub-10 nm Wires"

May 28-30, 2008

Y. Hasegawa, F. Komori, Y. Kuk, Q. Xue, J. Yoshinobu, and S. Hasegawa

Electronic states and transport in molecules and nanowires have recently attracted much attention. The aim of the present international spring school was to introduce fundamental knowledge on physics and chemistry of low-dimensional electronic systems for young researchers in this interdisciplinary field of nanoscience. It was co-organized by A3 Foresight Program "Sub-10 nm Wires" and ISSP.

The school consisted of the following three lectures on electronic states and transport properties in low dimensional systems, and a poster session.

- (A) Quantum Transport
Professor Tsuneya Ando (Tokyo Institute of Technology)
Over view and details of theoretical approaches on the quantum transport were given with a focus on carbon nanotubes and a few layer graphenes.
- (B) Quantum Physics of Thin Metal Films
Professor Tai-Chang Chiang (University of Illinois)
Quantization of the electron energy levels in metallic thin films was discussed from the principle of photoelectron spectroscopy to the detailed analyses of interface scattering.
- (C) Fundamentals of Nanoelectronics
Professor Supriyo Datta (Purdue University)
Fundamentals and his original methods on quantum transport were given including advanced discussion on spin transport and energy dissipation.

More than 200 students (51 from abroad) attended the lectures, and 50 posters were presented. This school was financially supported by JSPS, NSFC, KOSEF and ISSP.



Supercomputing in Solid State Physics 2009

February 16-19, 2009

N. Kawashima, H. Noguchi, O. Sugino, T. Suzuki, Y. Tomita, S. Tsuneyuki, and Y. Yoshimoto

Every year, we host a domestic workshop in which most of the heavy users of the ISSP supercomputers get together and exchange new ideas. At the end of the school year 2008, the present supercomputer system is finishing its 4th year of the current 5 year lease contract. We considered that this would be a good opportunity to have an international event by extending our annual workshop, in order to review most important recent results in computational physics and stimulate further developments in both methodology and applications. With this background, we invited 40 speakers including 12 from overseas. In addition to the oral presentations by the invited speakers, there are 46 poster presentations. Everyday we had audience of 80-90 who participated in lively discussions. Reflecting the diverse spectrum of the users of the ISSP supercomputer, a number of topics were picked up from various fields of physics, including hydrogen storage systems, ultra-cold atoms in laser traps, flow of blood cells, and even initial formation of the universe. In spite of this diversity, however, we discovered a lot of knowledge and techniques that are, or can be, shared by many apparently different fields, which was one of the main objectives of the event.

URL: <http://www.issp.u-tokyo.ac.jp/public/scissp/>

Charge Fluctuation and Nonlinear Conduction of Molecular Conductors

May 21, 2008

I. Terasaki, Y. Nogami, M. Ogata, H. Seo, T. Kato, and H. Mori

Nonlinear conduction of charge-ordered molecular conductors is a hot topic in these days. Owing to the electric field response of charge fluctuation, the threshold voltage is low, so that the intrinsic non-equilibrium state can be studied. As a result, the dc-ac converter (synchronization) as an organic thyristor and the appearance of the metastable state, namely key words of non-equilibrium system, have been observed. In this workshop, the recent progress of experimental and theoretical results, development of materials, dynamical crystal structure analyses under electric field, optical measurements, time-resolved nonlinear conduction, nonlinear conduction under magnetic field, theoretical studies of nonlinear conduction, etc., has been discussed. More than 66 researchers have joined and had hot discussions. The participants commented that this workshop is very educational about recent progress of nonlinear conduction. We hope that this fruitful workshop triggers the new development of our researches.

International Spring School on “Sub-10 nm Wires”

May 28-30, 2008

F. Komori, Y. Hasegawa, J. Yoshinobu, Y. Kuk, Q. Xue, and S. Hasegawa

This ISSP workshop was held as a part of the international workshop of the same title. The school consisted of the three lectures on electronic states and transport properties in low dimensional systems, and a poster session by the participants. The details are given in the section of “International Conferences and Workshops”.

Recent Developments in the Physics of Heavy Fermions

July 23-25, 2008

T. Sakakibara, Y. Onuki, T. Takabatake, Y. Matsuda, H. Harima, T. Hotta, and H. Sato

Heavy-fermion systems have been extensively studied since the discovery in late 1970's. It is now well established that the Kondo effect of spin origin and the magnetic quantum criticality are important ingredients of the heavy-fermion states. This “classical” view of heavy fermions has recently been challenged by the discovery of f-electron compounds whose mass enhancement is quite immune to strong magnetic fields. This suggests a new mechanism for the formation of heavy fermions possibly arising from multipole degrees of freedom and/or a rattling motion of atoms. This workshop was organized to bring together researchers working in this field to discuss various new aspects of the heavy-fermion physics as well as new developments in experimental techniques. Topics discussed in the workshop included dHvA and PES experiments on heavy fermions, heavy-fermion superconductors, multipole orderings and fluctuations, rattling properties, heavy-fermion theories and new materials. We had 245 participants in total, and 45 oral and 25 poster presentations were given in the workshop.

Supercomputing in Solid State Physics 2009

February 16-19, 2009

N. Kawashima, H. Noguchi, O. Sugino, T. Suzuki, Y. Tomita, S. Tsuneyuki, and Y. Yoshimoto

See the section of “International Conferences and Workshops”.

The 2nd Workshop on the Science and Technology Based on the Advanced Coherent Light Sources: “Progress of Photon Science at Extreme Wavelengths”

March 2-3, 2009

T. Suemoto

The laser based coherent light sources in the extreme ultraviolet and soft X ray regions have been developed at ISSP, Riken, JAEA and some other research institutes in Japan. The available photon energy is now extended to several hundreds electron volts at the high energy side and the shortest pulse width reaches in the range of one hundred attoseconds. High photon flux and high stability are achieved and the new innovative technologies such as fiber lasers accelerate the field. Using these newly developed laser light sources, novel spectroscopic methods such as attosecond molecular spectroscopy, high resolution photoelectron spectroscopy, inner shell non-linear spectroscopy, ultrafast imaging are proposed and some of them are demonstrated. In order to take initiative in this new field of photon science and widen the application, ISSP and the Graduate School of Frontier Sciences propose an establishment of “Advanced Coherent Light Laboratory” at Kashiwa campus. This workshop has been organized to present this Kashiwa plan to the large audience outside the university and to encourage the development of this new field by the close collaboration among the laser engineers, solid state physicists and synchrotron users. Twenty presentations are given in the sessions (1) Short wavelength lasers and their prospects (2) Research using short wavelength lasers, (3) From synchrotron radiation to lasers (4) From visible to shorter wavelengths (5) Exploration of new physics. During the free discussion time, four talks initiated discussions on the necessity of a middle scale facility for photon science. The total number of attendants on the first and the second day amounted to 130.

Design and Sciences of the KEK-Todai Chopper Spectrometer Project

March 18, 2009

T. J. Sato

The neutron science laboratory of the institute for solid state physics (ISSP-NSL) has been promoting the user program as well as its own research programs using the JRR-3 research reactor. On the other hand, there is an on-going effort to realize an intense spallation neutron source, J-PARC/MLF, just beside the reactor, which will be fully operational in very near future. On this occasion of achieving two different-type sources, ISSP-NSL has initiated construction of a chopper spectrometer at the spallation source, jointly with the neutron science laboratory of the high-energy accelerator research organization (KEK-KENS).

The chopper spectrometer covers wide E-Q range with realizing high-energy-resolution and high-counting-rate modes by selecting suitable chopper devices for the different necessities. It is partly based on the HRC spectrometer of KEK-KENS, which has been under construction, and on VINS which has been planned by ISSP-NSL. In this workshop, we discuss the spectrometer specifications of the joint project, as well as possible scientific opportunities that can be enabled by its enlarged capability.

